Shinq-Jen Wu, et.al. International Journal of Engineering Research and Applications
www.ijera.com
ISSN: 2248-9622, Vol. 15, Issue 8, August 2025, pp 67-88

RESEARCH ARTICLE OPEN ACCESS

Block-Diagram Implementation of S-system Sensitivity Analysis: A Simulink Framework for Power-Law Biological Networks

Shinq-Jen Wu[1,*] andSing-Yu Lu[2]

[1,2] *Department of Electrical Engineering Da-Yeh University, 168 University Rd., Dacun Changhua 51591, Taiwan, R.O.C*

Abstract

S-system models, characterized by their inherent power-law formalism, offer a powerful framework for modeling large-scale biological systems due to their ability to represent complex interactions through simplified algebraic structures. While steady-state solutions and their associated sensitivities can be derived analytically through algebraic equations, the dynamic response of S-systems to perturbations in both environmental conditions (independent variables) and intrinsic parameters (e.g., tissue-specific kinetic properties) remains an open research challenge.This study specifically addresses this gap by developing a novel approach to analyze the dynamic sensitivity of S-systems, with two primary objectives: Quantify the instantaneous system response to perturbations in rate constants and kinetic exponents.Identify critical parameters governing transient behaviors. Leveraging the unique mathematical properties of power-law systems, we reformulate the dynamic sensitivity as a differential matrix equation featuring a diagonal parametric matrix, which is subsequently simplified through rigorous matrix operations.To enhance accessibility for biological researchers, we implement the entire analytical framework within Simulink (MATLAB's graphical modeling environment). The Simulink creates an intuitive visual interface thatrepresents complex matrix operations as modular blocks, enables real-time perturbation analysis, and facilitates parameter importance ranking through interactive visualization**.**

Keywords: computational analysis, computational biology, graphical models, biochemistry, systems biology

---

Date of Submission: 08-08-2025 Date of acceptance: 21-08-2025

I. INTRODUCTION

In this era where cancer instills widespread fear, the urgent priority is to mine high-throughput microarray data for system modeling and conduct in-depth dynamic behavior analysis. Bartocci and Lió (2016) reviewed computational modeling approaches, concluding that ODE-based system models effectively capture biological system behavior and will gain greater prominence [1]. Sriyudthsak et al. surveyed key models and applications in biochemical systems [2], while Voit provided a comprehensive review of Biochemical Systems Theory (BST), covering system model design, structure identification, parameter estimation (reverse engineering), steady-state diagnostics/computation, and BST applications to plant/animal systems and human physiology/disease – encompassing 752 studies [3].
S-systems in Eq. (1) quantify net interaction strengths between components.

$$\dot{x}_i = \underset{n+m}{f^i} = v_i^+ - v_i^- = \alpha_i \prod_{j=1}^{n+m} x_j^{g_{ij}} - \beta_i \prod_{j=1}^{n+m} x_j^{h_{ij}}, i = 1, \dots n \quad (1)$$

where v_i^+, v_i^- denote forward and reverse fluxes; $g_{ij}$and h_{ij}denote the *net interactive strength* fromx_j on x_i, α and $\beta_i$are the rate constants. The $x_i, i = 1, \dots n$are dependent variables and $x_{n+1}, \dots x_{n+m}$ are independent variables, the values of which remains constant during a period of an experiment.This power-law formalism offers exceptional versatility. In medium/large systems, the kinetic constants represent *net interaction strengths* rather than actual intensities. Real-valued (non-integer) exponents not only indicate relative influence strengths between key components but also interpret time-delay effects [4-6].S-system structure/parameter identification constitutes a multi-objectiveconstrained optimization problem. While computational intelligence techniques dominate this research area, most dry-lab tests only

validate small 3–5-dimensional systems with narrow search constraints. The complexity of structure identification often leads to conflation with simpler parameter estimation [7], selective small-system comparisons [6], or ambiguous methodologies [7].

Advances in High-Dimensional Identification

Kimura et al. and Prof. Feng-Sheng Wang (National Chung Cheng University) rigorously addressed 30-dimensional systems but were limited by contemporary techniques in identifying weak connections Crucially, in medium/large systems these kinetic constants represent *relative strengths* rather than absolute interaction values, necessitating broader parameter bounds beyond 4 reaction orders.During 2010–2018, we advanced this field by developing AI techniques with expanded bounds[8-12], and creating novel computational methods: (a) Self-adaptive multi-objective optimization via fuzzy inference [8], (b) Enhanced algorithms: EEGA (Exploration-Exploitation GA) [8], sDE (optimized differential evolution) [9], hLS (heuristic deviation-based local search) [9], (c) Bio-inspired hybrids: CGA (Cockroach-competitive GA) [10], SCGA (Seed Strategy/Chemotaxis-based GA) [11], (d) Cockroach Swarm Evolution (CSE) [12]. These successfully achieved structure identification and parameter estimation for30-gene S-systems.For large-system data mining, feature selection identifies 30 core genes, whose time-series data reconstructs nonlinear dynamic models of gene regulatory interactions. Such models should suffice to predict dynamic behaviors in large biological systems (e.g., cancer mechanisms). Consequently, our recent work shiftsfocus to*relative stability* (root-locus-based stability analysis for Michaelis-Menten kineticsmodules [13] and Leveraging S-systems' power-law structure to simplify steady-state value and sensitivity calculations via algebraic solutions [14, 15]), and *dynamic sensitivity* analysis (directly analyzing transient behavior sensitivity).

Current Focus: Stability and Sensitivity Analysis

Sensitivity analysis systematically investigates how systems respond to perturbations in inputs or parameters. Time-varying parametric sensitivity analysis (dynamic sensitivity) quantifies structural uncertainties arising from parameter variations, enhancing our understanding of system dynamics and enabling identification of bottleneck enzymes—critical reaction steps that govern system behavior. Chen et al. develop a single-cell-resolution sensitivity framework linking parameter perturbations to phenotypic heterogeneity in cancer and identify three dynamical regimes of parameter influence [16].Recent advances in dynamic sensitivity analysis (Zi, 2021) have enabled the decomposition of transient biological behaviors into parameter-specific contributions, overcoming limitations of traditional steady-state approaches [17].Two primary approaches exist:

1. *Global Sensitivity Analysis*: Examines system responses to simultaneous, large-scale parameter variations using methods like variance-based analysis, moment-independent techniques, and functional principal component analysis (FPCA). FPCA has revealed key features in insulin signaling pathways [18], while other applications include hazard reduction in debris flows [19].
2. *Local Sensitivity Analysis*: Focuses on infinitesimal perturbations of individual parameters. Hu and Yuan successfully applied this to MAPK/PI3K signaling pathways [20], though it requires solving coupled sensitivity and system ODEs—a challenge addressed by:Wu et al.'s modified collocation methods with Lagrange polynomials [21], Shiraishi et al.'s Taylor-series-based SoftCADs software [22, 23],Perumal and Gunawan's pathway-specific perturbation analysis [24].

Normalized dynamic sensitivity (logarithmic gain) further refines this analysis, proving effective for identifying metabolic bottlenecks in ethanol fermentation [25, 26] and aromatic amino acid biosynthesis [27]. Building on these advances, our study employs block-diagram visualizations of coupled system/sensitivity ODEs to compute local dynamic parametric sensitivities [28].

Biological systems exhibit complex nonlinear dynamics that require sophisticated mathematical frameworks for analysis. Among these, ***S-systems*** (a canonical power-law formalism within Biochemical Systems Theory, BST)offer unique advantages for modeling biological networks through their structured representation of interactions as products of power-law functions [3]. Complementing Michaelis-Menten kinetics (widely used for enzyme-catalyzed reactions), S-systems provide a unified framework for modeling metabolic, genetic, and signaling pathways with inherent scalability and analytical tractability [29]. While both frameworks are pillars of computational systems biology, extracting insights from their dynamic behavior demands rigorous *sensitivity analysis* to quantify how perturbations propagate through these networks.Traditional sensitivity methods often struggle with the *high-dimensional, nonlinear, and time-varying nature* of biological models. Dynamic sensitivity analysis—which captures transient responses rather than just steady-state behavior—is particularly crucial for identifying critical parameters governing system robustness, bifurcations, and cellular decision-making [30].

However, implementing such analyses for S-systems presents computational challenges due to*complex coupling* between power-law terms,*state-dependent parametric influences* and the curse of dimensionality in large networks. Thomos (2022) demonstrates how traditional steady-state sensitivity metrics fail to capture transient pathway activation, oscillatory behaviors (e.g., circadian rhythms) and bifurcation thresholds in cell fate decisions [31].

Visualization tools like **Simulink** (a MATLAB-based graphical modeling environment) offer promising solutions. As demonstrated in our prior work on Michaelis-Menten kinetics (Wu et al., 2022), Simulink enables intuitive block-diagram representations of differential equations and their sensitivity counterparts. By decomposing large systems into modular subsystems, Simulink facilitates*real-time visualization* of parameter-state interactions,*efficient computation* of sensitivity trajectories and *integration of local/global sensitivity metrics* (e.g., L_1/L_2 norms) for transient dynamics [28].While this approach proved effective for Michaelis-Menten modules, its extension to S-systems remains unexplored. This gap is significant given S-systems' broader applicability to non-enzymatic networks (e.g., gene regulation, metabolic pathways) and their analytical advantages for steady-state and stability analysis [32].Here, we bridge this gap by developing a *Simulink-based framework for dynamic sensitivity analysis of S-systems*. The dynamic sensitivity analysis of S-systems is reformulated into a differential matrix equation incorporating a *diagonal parameter matrix*. Subsequent simplification is achieved via structured matrix operations. These processes are implemented and visualized using MATLAB's Simulink environment, offering a model-based interface suitable for systems biology applications.By unifying the analytical power of S-systems with Simulink's computational flexibility, this work provides a scalable toolkit for probing biological robustness, identifying design principles, and accelerating rational intervention strategies.

II. METHODS

Perturbation Theorem for S-system Parametric Sensitivity Analysis

Given a nonlinear system:$\dot{X}(t) = F(X(t), t, \boldsymbol{\theta}^0),\ X(t_0) = X_0$, where state variable$X(t) = [x_1, \dots x_n]^T$,parameter vectors $\boldsymbol{\theta} = [\theta_1, \dots \theta_m]^T \in R^m$, nominal solution $\varphi^0(t)$ (parametrized by t_0, X_0 and $\boldsymbol{\theta}^0$). Under parameter perturbation$\boldsymbol{\theta}^0 \to \boldsymbol{\theta}^0 + \delta\boldsymbol{\theta}$,the perturbed solution$\varphi^0 + \delta\varphi$ satisfies [33]:

$$\dot{\varphi}^0(t) + \delta\dot{\varphi}(t) = F(\varphi^0 + \delta\varphi, t, \boldsymbol{\theta}^0 + \delta\boldsymbol{\theta}) = F(\varphi^0, t, \boldsymbol{\theta}^0) + D_1F|_{(\varphi^0,t,\boldsymbol{\theta}^0)} \cdot \delta\varphi + D_3F|_{(\varphi^0,t,\boldsymbol{\theta}^0)} \cdot \delta\boldsymbol{\theta} + H.O.T.. \quad (2)$$

Let $D_iF|_{(\varphi^0,t,\boldsymbol{\theta}^0)}, i = 1,3$denote the partial derivative of F with respect to its ith argument—$i = 1$for the state variables φ and $i = 3$ for the parameters $\boldsymbol{\theta}$. Neglecting higher-order terms in $\delta\varphi$ and $\delta\boldsymbol{\theta}$,the system is approximated by

$$\delta\dot{\varphi}(t) = D_1F|_{(\varphi^0,t,\boldsymbol{\theta}^0)} \cdot \delta\varphi + D_3F|_{(\varphi^0,t,\boldsymbol{\theta}^0)} \cdot \delta\boldsymbol{\theta}. \quad (3)$$

Defining the parametric dynamic sensitivity as$S = \frac{\delta\varphi}{\delta\boldsymbol{\theta}}$, we obtain the sensitivity equation:

$$\frac{dS(t)}{dt} = A(t)S(t) + B(t), \quad (4)$$

wherethe Jacobian matrix$A(t) = D_1F|_{(\varphi^0,t,\boldsymbol{\theta}^0)} = \left[\frac{\partial f_i}{\partial x_j}\right]_{\substack{i=1,\dots n \\ j=1,\dots n}}$, $B(t) = D_3f|_{(\varphi^0,t,\boldsymbol{\theta}^0)}, S(0) = 0.$

S-system Sensitivity Analysis

For thebiologicalS-system,as shown in Eq. (1), the parametric dynamic sensitivity$S(t) = \begin{bmatrix} u^1 & 0 & 0 \\ 0 & \ddots & 0 \\ 0 & 0 & u^n \end{bmatrix}_{n\times\boldsymbol{P}}$, the Jacobian matrix$A(t) = \begin{bmatrix} a_1 \\ \vdots \\ a_n \end{bmatrix}, B(t) = \begin{bmatrix} b_1 & 0 & 0 \\ 0 & \ddots & 0 \\ 0 & 0 & b_n \end{bmatrix}_{n\times\boldsymbol{P}}$ and$\boldsymbol{P} = [p^1 \cdots p^n]$ where $p^i, i = 1 \cdots n$ denotes the number of the parameters related to $\dot{x}_i$in Eq. (1),

$$u^i = \left[\frac{\partial x_i}{\partial \alpha_i}, \frac{\partial x_i}{\partial \beta_i}, \frac{\partial x_i}{\partial g_{i1}} \cdots \frac{\partial x_i}{\partial g_{i,n+m}}, \frac{\partial x_i}{\partial h_{i1}} \cdots \frac{\partial x_i}{\partial h_{i,n+m}}\right],$$

$$a_i = [a_{i1} \dots a_{in}] = [\tfrac{\partial f_i}{\partial x_1} \tfrac{\partial f_i}{\partial x_2} \cdots \tfrac{\partial f_i}{\partial x_n}] = [\tfrac{1}{x_1}(g_{i1}v_i^+ - h_{i1}v_i^-) \cdots \tfrac{1}{x_n}(g_{in}v_i^+ - h_{in}v_i^-)],$$

$$b_i = \left[\frac{\partial f_i}{\partial \alpha_i}, \frac{\partial f_i}{\partial \beta_i}, \frac{\partial f_i}{\partial g_{i1}} \cdots \frac{\partial f_i}{\partial g_{i,n+m}}, \frac{\partial f_i}{\partial h_{i1}} \cdots \frac{\partial f_i}{\partial h_{i,n+m}}\right] = \left[\frac{v_i^+}{\alpha_i}, \frac{-v_i^-}{\beta_i}, v_i^+ \ln x_1 \cdots v_i^+ \ln x_{n+m}, -v_i^- \ln x_1 \cdots -v_i^- \ln x_{n+m}\right]. \quad (5)$$

Through matrix analysis, we know $a_{ij} \cdot u^j = 0$ for all $i \neq j$:

$$a_{ij} \cdot u^j = \frac{\partial f_i}{\partial x_j} \cdot \left[\frac{\partial x_j}{\partial \alpha_i}, \frac{\partial x_j}{\partial \beta_i}, \frac{\partial x_j}{\partial g_{i1}} \cdots \frac{\partial x_j}{\partial g_{i,n+m}}, \frac{\partial x_j}{\partial h_{i1}} \cdots \frac{\partial x_j}{\partial h_{i,n+m}}\right] = \left[\frac{\partial f_j}{\partial \alpha_i}, \frac{\partial f_j}{\partial \beta_i}, \frac{\partial f_j}{\partial g_{i1}} \cdots \frac{\partial f_j}{\partial g_{i,n+m}}, \frac{\partial f_j}{\partial h_{i1}} \cdots \frac{\partial f_j}{\partial h_{i,n+m}}\right] = 0.$$

The equation in Eq. (5) can be further simplified to a diagonal matrix form in Eq. (6) with $\bar{p} = \max(p^i)$:(For generalization we use zero to fill the elements for$p^i < \bar{p}$.)

$$d\hat{S}(t)/_{dt} = \hat{A} \cdot \hat{S} + \hat{B}, \qquad (6)$$

Where$\hat{S}(t) = \begin{bmatrix} u^1 \\ \vdots \\ u^n \end{bmatrix}_{n\times\bar{p}}$, $\hat{A} = \begin{bmatrix} a_{11} & 0 & 0 \\ 0 & \ddots & 0 \\ 0 & 0 & a_{nn} \end{bmatrix}_{n\times n}$ with $a_{ii} = \frac{\partial f_i}{\partial x_{1i}} = \frac{g_{ii}\cdot v_i^+ - h_{ii}\cdot v_i^-}{x_i}, i = 1 \cdots n$ and $\hat{B} = \begin{bmatrix} b^1 \\ \vdots \\ b^n \end{bmatrix}_{n\times\bar{p}}$.

The related scalar parametric dynamic sensitivity for $\alpha_i, \beta_i, g_{il}, h_{im}$:

$$\frac{dS_{i1}}{dt} = \left(a_{ii} \cdot S_{i1} + \frac{v_i^+}{\alpha_i}\right), \quad for\ \alpha_i,$$

$$\frac{dS_{i2}}{dt} = \left(a_{ii} \cdot S_{i2} + \frac{-v_i^-}{\beta_i}\right), \quad for\ \beta_i,$$

$$\frac{dS_{il}}{dt} = \frac{1}{x_i}(a_{nii} \cdot S_{il} + v_i^+ \cdot \ln x_l), \quad for\ g_{il},$$

$$\frac{dS_{im}}{dt} = \frac{1}{x_i}(a_{ii} \cdot S_{im} - v_i^- \cdot \ln x_m), \quad for\ h_{im}, \qquad (7)$$

Considering that the scales of different components may vary significantly, we further normalize the sensitivity using the form$S_{nij} = \frac{\partial x_i/x_i}{\partial \theta_j/\theta_j}$ and let$a_{nii} = g_{ii} \cdot v_i^+ - h_{ii} \cdot v_i^-$: (for $i = 1 \cdots n$)

$$\frac{dS_{ni1}}{dt} = \frac{1}{x_i}(a_{nii} \cdot S_{ni1} + v_i^+), \quad for\ \alpha_i,$$

$$\frac{dS_{ni2}}{dt} = \frac{1}{x_i}(a_{nii} \cdot S_{ni2} - v_i^-), \quad for\ \beta_i,$$

$$\frac{dS_{nil}}{dt} = \frac{1}{x_i}(a_{nii} \cdot S_{nil} + g_{il} \cdot v_i^+ \cdot \ln x_l), \quad for\ g_{il},$$

$$\frac{dS_{nim}}{dt} = \frac{1}{x_i}(a_{nii} \cdot S_{nim} - h_{im} \cdot v_i^- \cdot \ln x_m), \quad for\ h_{im}. \qquad (8)$$

A corresponding block diagram of the S-system is then constructed in the Simulink environment to provide the dynamic values of the state variables x_i as well as their associated forward and reverse fluxesv_i^+, v_i^-. This setup enables the extraction of the normalized dynamic sensitivity $S_{nij} = \frac{\partial x_i/x_i}{\partial \theta_j/\theta_j}$.

Block Diagram-based Visualization

Simulink (MathWorks®) is a computational modeling environment that implements a block diagram paradigm for dynamic system analysis [33]. In this framework,biological components are abstracted as functional blocks and directed signal lines encode dynamic interactions (e.g., metabolic fluxes, regulatory signals).Dynamic Sensitivity Analysis (native tools for parametric sensitivity computation), multi-domain simulation (unified modeling of biochemical reaction networks, control theoretic constructs and stochastic processes) and*visual analytics* (real-time visualization of state variable trajectories and parameter influence metrics) are available.Biological applicationsfor transient response analysis in ODE-based biological models, bottleneck identification in metabolic pathways and optimization of kinetic parameters through interactive perturbation are achievable. The graphical interface eliminates low-level programming requirements while maintaining mathematical rigor through automated Jacobian computation for sensitivity matrices, adaptive solvers for stiff biological systems and exportable block libraries for modular network design.

III. RESULTS and DISCUSSION

S-system models provide a powerful framework for analyzing biological networks through their canonical power-law formalism (Eq. 1), where system dynamics emerge from coupled synthesis and degradation terms. While analytical solutions exist for steady-state sensitivity [14, 15], understanding time-varying parameter influences remains challenging, particularly for capturing transient behaviors during system perturbations. This study develops a Simulink-based computational platform that: (a) Preserves modular

interpretability through block-matrix formulations, (b)Visualizes dynamic sensitivity propagation through modular block diagrams, (b) Quantifies parameter dominance across different time regimes (immediate/transient/steady-state), (c) Identifies critical parameters controlling system reconfiguration.

By implementing the sensitivity matrix equations $d\hat{S}(t)/_{dt} = \hat{A} \cdot \hat{S} + \hat{B}$) as customizable Simulink blocks, we enable interactive exploration of how kinetic parameters ($\alpha_i, \beta_i, g_{ij}, h_{ij}$) govern system reconfiguration—without requiring analytical derivations for each new model.Focusing on canonical S-system modules, we demonstrate how sensitivity dynamics emerge from the interplay between kinetic exponents and rate constants—revealing design principles applicable to larger networks.

■ Visualize Parametric Dynamic Sensitivity

To demonstrate the proposed approach, we consider a small-scale S-system representing a cascade pathway (Figure 1) [34].

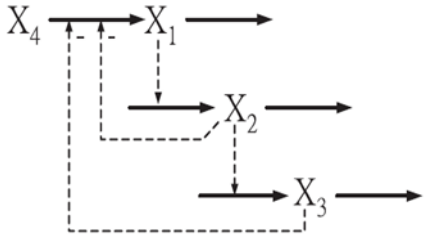

Figure 1: Three-tier cascade pathway [34]

For a small-scale system, experimental data can be used to directly determine the excitatory and inhibitory relationships between its constituents (e.g., genes, proteins, or metabolites). Figure 1 illustrates a three-step cascade pathway featuring two negative feedback loops. The system comprises three dependent constituents(x_1, x_2, x_3) and one constant sourcex_4, which is an independent constituent.The constituent x_1 is produced from x_4 , and this production is inhibited by both x_2 and x_3 .The generated x_1 then induces the production of x_2 , which further promotes the generation of x_3 .All constituents undergo self-degradation over time.Based on this pathway, the corresponding S-system is formulated as follows:

$$\begin{aligned} \dot{x}_1 &= 10x_2^{-0.1}x_3^{-0.05}x_4 - 5x_1^{0.5}, \\ \dot{x}_2 &= 2x_1^{0.5} - 1.44x_2^{0.5}, \\ \dot{x}_3 &= 3x_2^{0.5} - 7.2x^{0.5}. \end{aligned} \quad (9)$$

The exponent orders and rate constants are adopted from Tsai and Wang's study [34]. In typical conditions, the concentration of the independent variable x_4 remains constant. The system possesses three dependent variables and one independent variable ($n = 3, m = 1$). There are thirty parameters: $\alpha_i, \beta_i, i = 1, \cdots 3$ and $g_{ij}, h_{ij}, i = 1, \cdots 3, j = 1, \cdots 4$. The parametric dynamic sensitivity in Eq. (1) is ($\frac{dS(t)}{dt} = A(t)S(t) + B(t)$ with the size of $S(t)_{3\times30}$, the Jacobian matrix $A(t)_{3\times3}$ and $B(t)_{3\times30}$. Through matrix operation, The parametric dynamic sensitivity is simplified to a diagonal matrix form in Eq. (6) ($d\hat{S}(t)/_{dt} = \hat{A} \cdot \hat{S} + \hat{B}$) with the size of $S(t)_{3\times6}$ ($\bar{p} = \max(p^i) = \max(6,4,4)$), the Jacobian matrix $A(t)_{3\times3}$ and $B(t)_{3\times6}$. The corresponding non-zero scalar form for the cascade system has only fourteen scalar equations in Eq. (7).For the state variable $x_1$only the sensitivity of x_1 to the parameters $\alpha_1, \beta_1, g_{12}, g_{13}, h_{11}$ is nonzero. In the case of infinitesimal perturbation, we have the following dynamic sensitivity equation of the reversible system, wherein $S_n^1 = (S_{n11}, S_{n12}, S_{n13}, S_{n14}, S_{n15})$ and $S_{n1i}, i = 1, \ldots 5$ denote the normalized sensitivity of $x_1$to the parameters $\alpha_1, \beta_1, g_{12}, g_{13}, h_{11}$,respectively:

$$\begin{aligned} \frac{dS_{n11}}{dt} &= \frac{1}{x_1}(a_{n11} \cdot S_{n11} + v_1^+), \quad for\ \alpha_1, \\ \frac{dS_{n12}}{dt} &= \frac{1}{x_1}(a_{n11} \cdot S_{n12} - v_1^-), \quad for\ \beta_1, \\ \frac{dS_{n13}}{dt} &= \frac{1}{x_1}(a_{n11} \cdot S_{n13} + g_{12} \cdot v_1^+ \cdot \ln x_2), \quad for\ g_{12}, \\ \frac{dS_{n14}}{dt} &= \frac{1}{x_1}(a_{n11} \cdot S_{n14} + g_{13} \cdot v_1^+ \cdot \ln x_3), \quad for\ g_{13}, \\ \frac{dS_{n15}}{dt} &= \frac{1}{x_1}(a_{n11} \cdot S_{n15} - h_{11} \cdot v_1^- \cdot ln\, x_1), \quad for\ h_{11}, \end{aligned} \quad (10)$$

where $a_{n11} = g_{11} \cdot v_1^+ - h_{11} \cdot v_1^-$ .For the state variable x_2 only the sensitivity of x_2 to the parameters $\alpha_2, \beta_2, g_{21}, h_{22}$ is nonzero. Let $S_n^2 = (S_{n21}, S_{n22}, S_{n23}, S_{n24})$ denotes the normalized sensitivity of x_2 to the parameters ($\alpha_2, \beta_2, g_{21}, h_{22}$):

$$\frac{dS_{n21}}{dt} = \frac{1}{x_2}(a_{n22} \cdot S_{n21} + v_2^+), \quad for\ \alpha_2,$$

$$\frac{dS_{n22}}{dt} = \frac{1}{x_2}(a_{n22} \cdot S_{n22} - v_2^-), \quad for\ \beta_2,$$
$$\frac{dS_{n23}}{dt} = \frac{1}{x_2}(a_{n22} \cdot S_{n23} + g_{21} \cdot v_2^+ \cdot \ln x_1), \quad for\ g_{21},$$
$$\frac{dS_{n24}}{dt} = \frac{1}{x_2}(a_{n22} \cdot S_{n24} - h_{22} \cdot v_2^- \cdot \ln x_2), \quad for\ h_{22}. \qquad (11)$$

where $a_{n22} = g_{22} \cdot v_2^+ - h_{22} \cdot v_2^- = -h_{22} \cdot v_2^-$. For the state variable x_3 only the sensitivity of x_3 to the parameters $\alpha_3, \beta_3, g_{32}, h_{33}$is nonzero. Let $S_n^3 = (S_{n31}, S_{n32}, S_{n33}, S_{n34})$ denotes the normalized sensitivity of x_3 to the parameters $(\alpha_3, \beta_3, g_{32}, h_{33})$:

$$\frac{dS_{n31}}{dt} = \frac{1}{x_2}(a_{n33} \cdot S_{n31} + v_3^+), \quad for\ \alpha_3,$$
$$\frac{dS_{n32}}{dt} = \frac{1}{x_2}(a_{n33} \cdot S_{n32} - v_3^-), \quad for\ \beta_3,$$
$$\frac{dS_{n33}}{dt} = \frac{1}{x_2}(a_{n33} \cdot S_{n33} + g_{32} \cdot v_3^+ \cdot \ln x_2), \quad for\ g_{32},$$
$$\frac{dS_{n34}}{dt} = \frac{1}{x_2}(a_{n33} \cdot S_{n34} - h_{33} \cdot v_3^- \cdot \ln x_3), \quad for\ h_{33}, \qquad (12)$$

where $a_{n33} = g_{33} \cdot v_2^+ - h_{33} \cdot v_2^- = -h_{33} \cdot v_2^-$.The differential equations in Eqs. (9), (10), (11) and (12) are further *visualized as four individual subsystems (shown in blocks) in Simulink environment*.

Figure 2 illustrates the normalized sensitivity block diagram for a serial reaction chain (subsystem shown)in Simulink environment. The S_n^ivisualized as a *single subsystem block* performs various perturbation response analysis (see the right-upper, right-middle and right-down blocks of Fig. 2). In Fig. 2, the left down subsystem (denoted as $\mathbb{S}$) visualizes the dynamic behavior of the cascadesystem in Eq. (9), the right upper subsystem (denoted as S_n^1) describes the dynamic normalized sensitivity of $x_1$in Eq. (10) and the rightmiddle subsystem (S_n^2) describes the dynamic normalized sensitivity of $x_2$in Eq. (11), and the right down subsystem (S_n^3) describes the dynamic normalized sensitivity of x_3 in Eq. (12). The system$\mathbb{S}$shares (V1+, V1-) denotingthe generation flux and consumption flux $(v_1^+,\ v_1^-)$ with x_1 sensitivity subsystem (denoted as S_n^1) , The system $\mathbb{S}$ shares (V2+, V2-) denotingthe generation flux and consumption flux $(v_2^+,\ v_2^-)$ with x_2 sensitivity subsystem (denoted as S_n^2). The system$\mathbb{S}$shares (V3+, V3-) denotingthe generation flux and consumption flux$(v_3^+,\ v_3^-)$ with x_3 sensitivity subsystem (denoted as S_n^2). The detailed block diagrams for system $\mathbb{S}$ and sensitivity $S_n^1, S_n^2$and $S_n^3$are shown in Figs. 3, 4, 5 and 6.The sensitivity to rate constants: $S_{ni1} = \frac{\partial x_i/x_i}{\partial \alpha_i/\alpha_i}$, $S_{ni2} = \frac{\partial x_i/x_i}{\partial \beta_i/\beta_i}$, $i = 1, \ldots 3$. The sensitivity to kinetic exponents: $S_{n13} = \frac{\partial x_1/x_1}{\partial g_{12}/g_{12}}, S_{n14} = \frac{\partial x_1/x_1}{\partial g_{13}/g_{13}}$, $S_{n15} = \frac{\partial x_1/x_1}{\partial h_{11}/h_{11}}$, $S_{n23} = \frac{\partial x_2/x_2}{\partial g_{21}/g_{21}}$, $S_{n24} = \frac{\partial x_2/x_2}{\partial h_{22}/h_{22}}, S_{n33} = \frac{\partial x_3/x_3}{\partial g_{32}/g_{32}}$, $S_{n34} = \frac{\partial x_3/x_3}{\partial h_{33}/h_{33}}$.

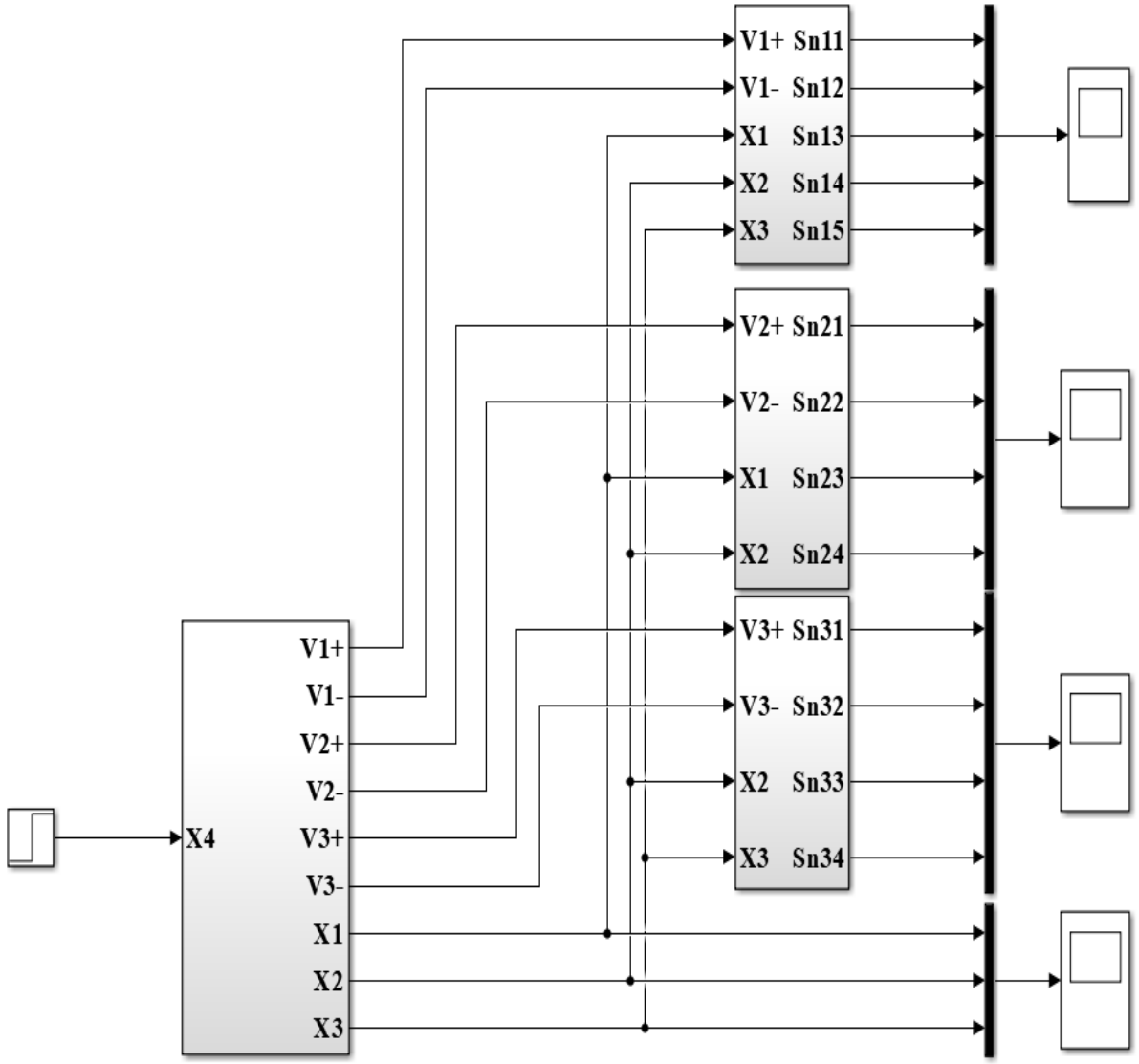

Figure 2: Visualize dynamic behavior and time-varying sensitivity in Simulink environment. The left down block runs the simulation of the reversible system (𝕊). The right upper block S_n^1, the right middle block $S_n^2$and the right down block $S_n^3$are for normalized dynamic sensitivity of x_1, $x_2$and x_3, respectively. The (Vi+, Vi-), i=1…3, denotethe generation flux and consumption flux$(v_i^+,\ v_i^-), i = 1 \ldots 3$.

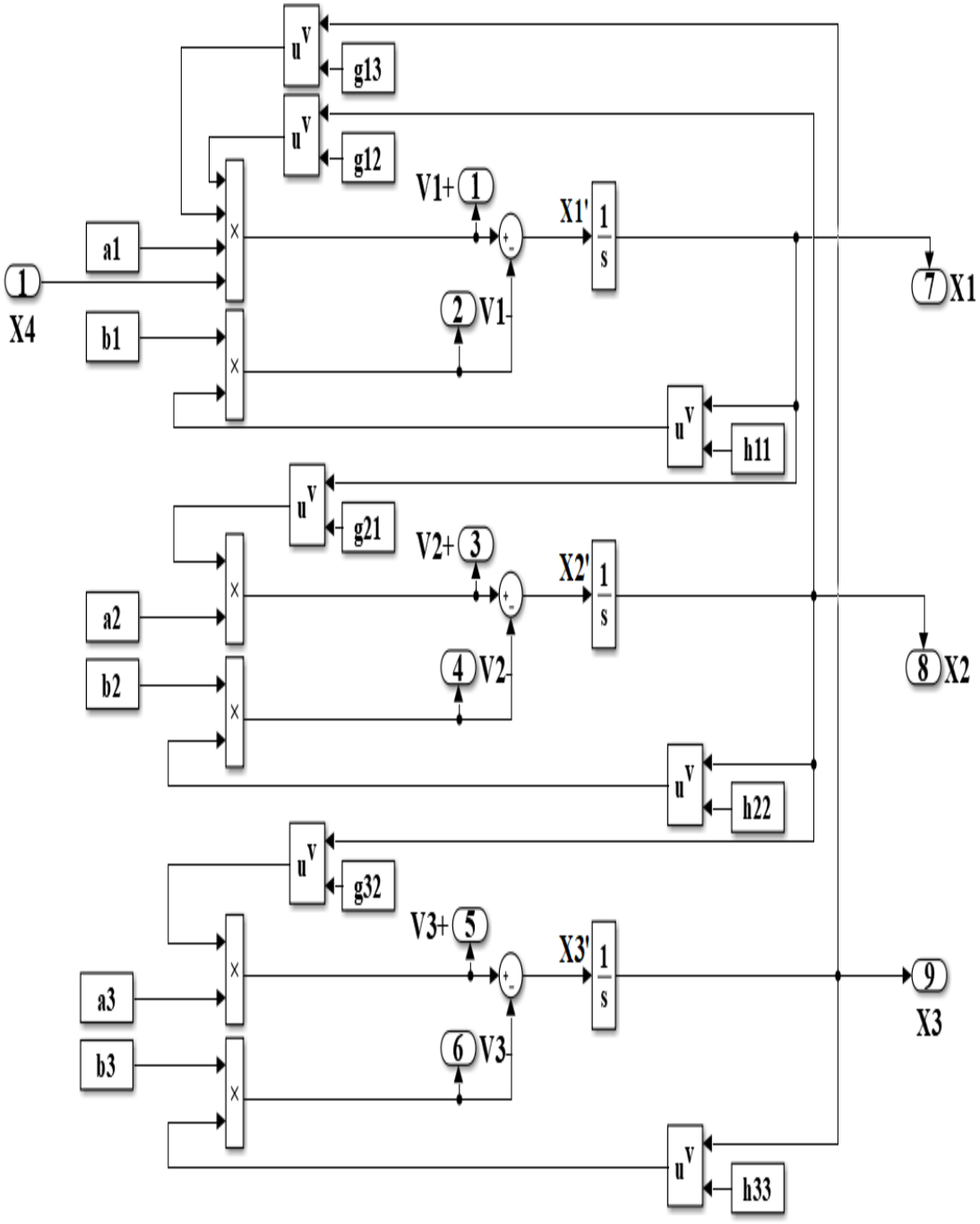

Figure 3: Detailed block diagram for the cascade system $\mathbb{S}$.

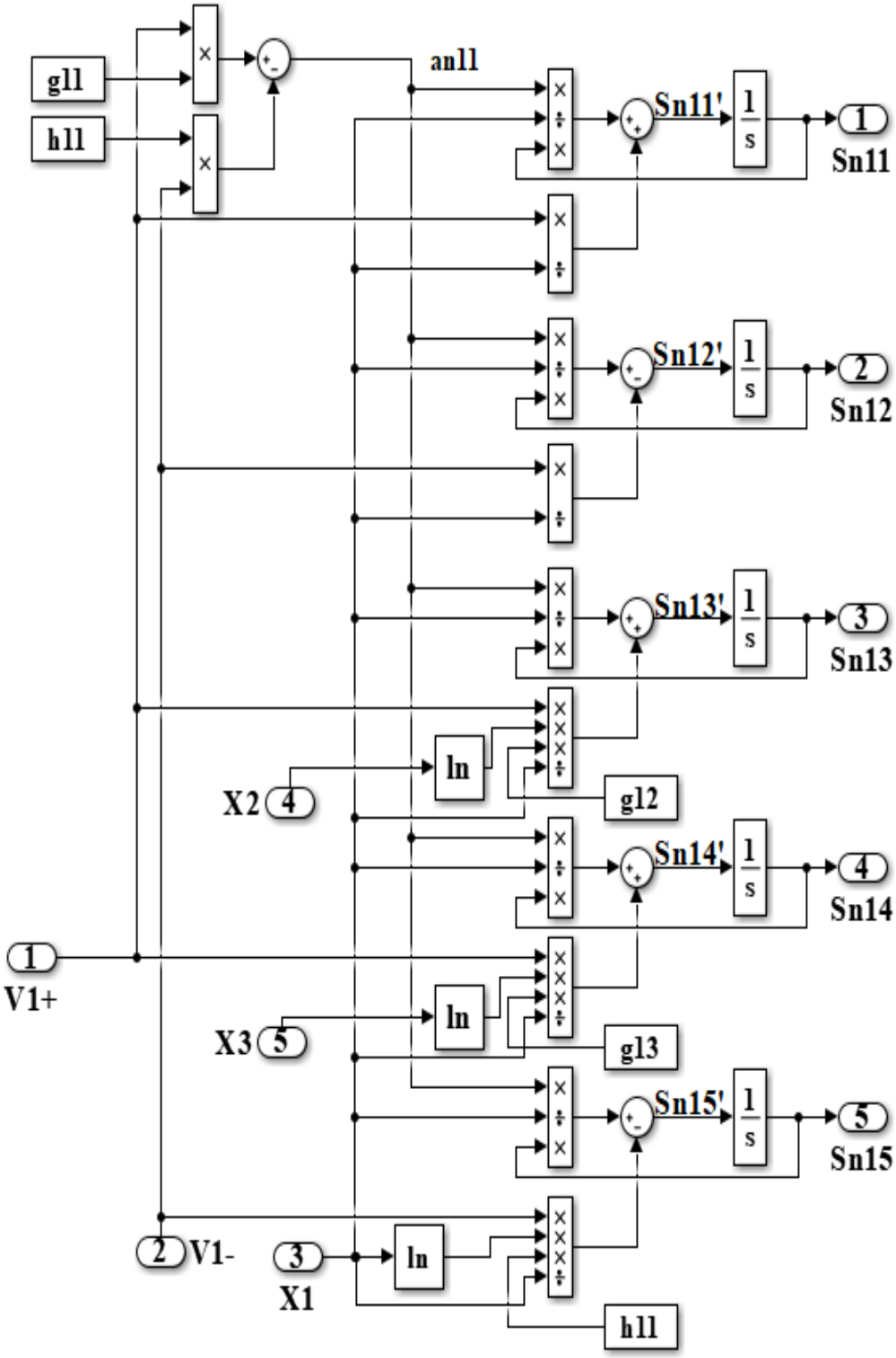

Figure 4: Detailed block diagrams for the dynamic sensitivity of x_1 (right upper block S_n^1 in Fig. 2). The sensitivity to rate constants is $S_{n11}=\frac{\partial x_1/x_1}{\partial \alpha_1/\alpha_1}$, $S_{n12}=\frac{\partial x_1/x_1}{\partial \beta_1/\beta_1}$. The sensitivity to kinetic exponents is $S_{n13}=\frac{\partial x_1/x_1}{\partial g_{12}/g_{12}} S_{n14}=\frac{\partial x_1/x_1}{\partial g_{13}/g_{13}}$, $S_{n15}=\frac{\partial x_1/x_1}{\partial h_{11}/h_{11}}$.

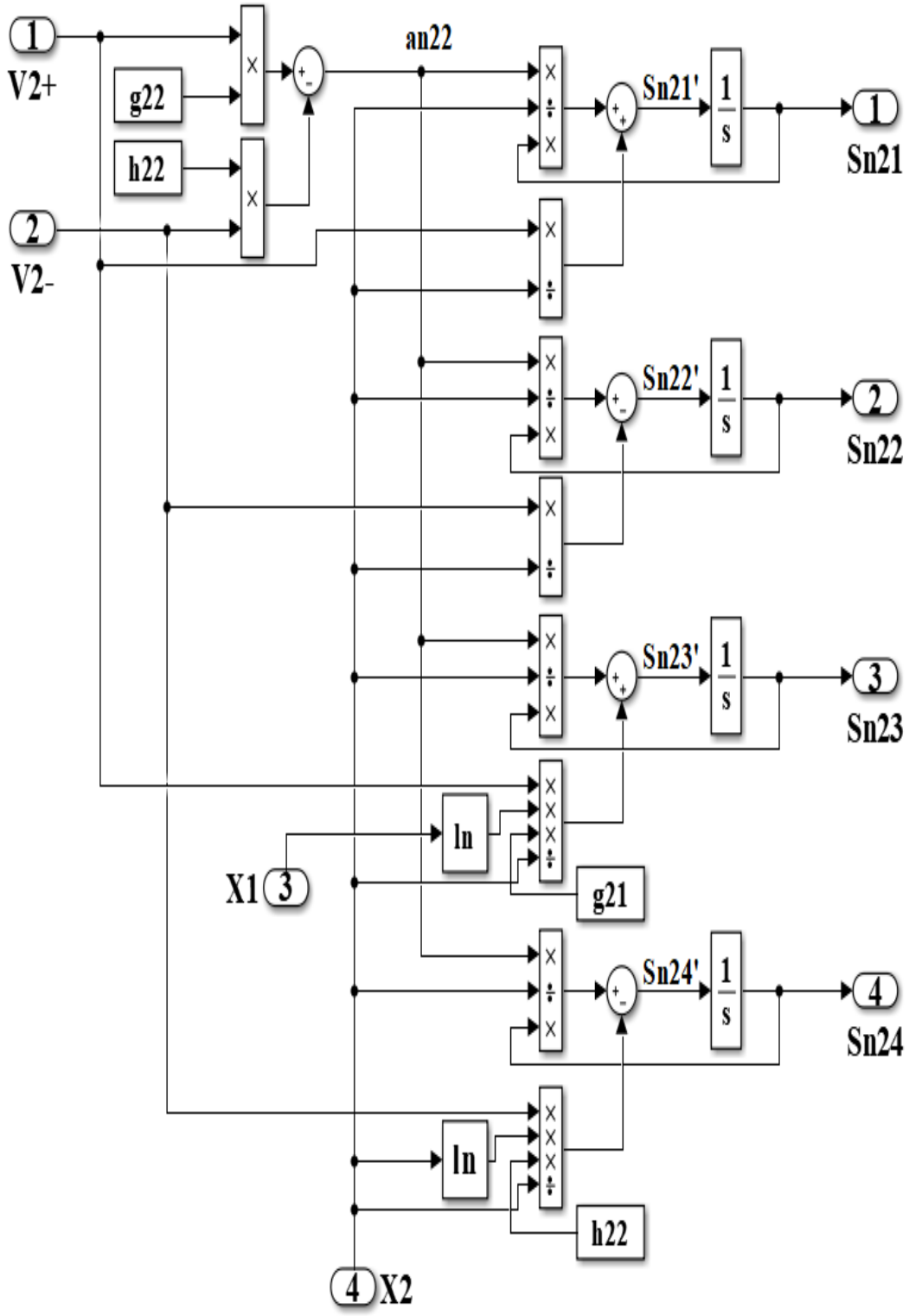

Figure 5: Detailed block diagrams for the dynamic sensitivity of x_2 (right middle block S_n^2 in Fig. 2).The sensitivity to rate constants is $S_{n21}=\frac{\partial x_2/x_2}{\partial \alpha_2/\alpha_2}$, $S_{n22}=\frac{\partial x_2/x_2}{\partial \beta_2/\beta_2}$. The sensitivity to kinetic exponents are $S_{n23}=\frac{\partial x_2/x_2}{\partial g_{21}/g_{21}}$, $S_{n24}=\frac{\partial x_2/x_2}{\partial h_{22}/h_{22}}$.

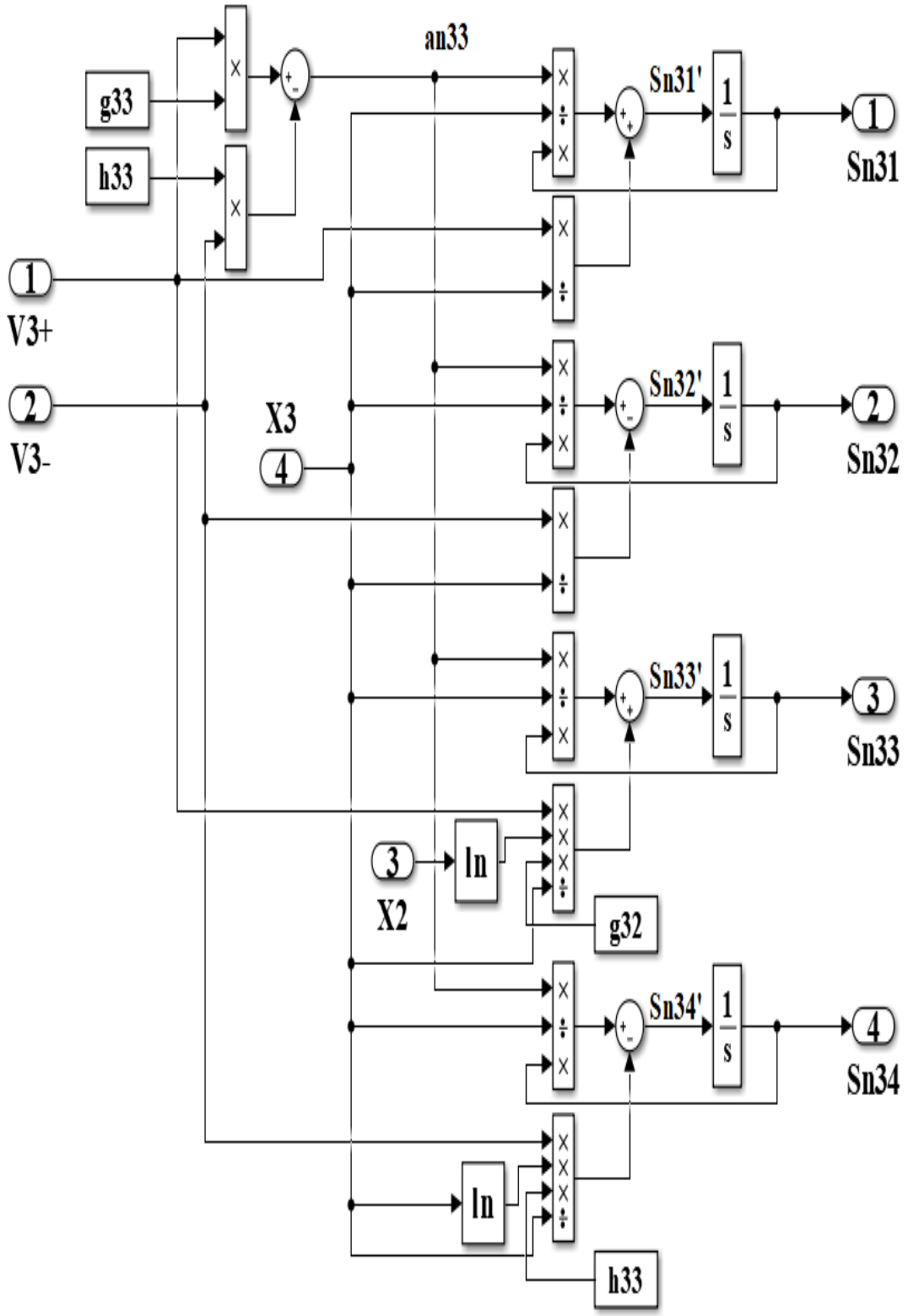

Figure 6: Detailed block diagrams for the dynamic sensitivity of x_3 (right down block S_n^3 in Fig. 2).The sensitivity to rate constants is $S_{n31}=\frac{\partial x_3/x_3}{\partial \alpha_3/\alpha_3}$, $S_{n32}=\frac{\partial x_3/x_3}{\partial \beta_3/\beta_3}$. The sensitivity to kinetic exponents are $S_{n33}=\frac{\partial x_3/x_3}{\partial g_{32}/g_{32}}$, $S_{n34}=\frac{\partial x_3/x_3}{\partial h_{33}/h_{33}}$.

Results of Dry Lab Experiments

The system was simulated under initial conditions (x_{10}, x_{20}, x_{30})= (0.2,0.5,0.1) with the independent variable fixed at $x_4 = 0.75$. As shown in **Figure 7**, the cascade system reaches steady state at t_s =10 seconds with equilibrium concentrations ($\bar{x}_1, \bar{x}_2, , \bar{x}_3$)= (1.8348, 3.5384, 0.6143).

***Key Observations from Sensitivity Analysis* (Figs. 8–10)**:

■ Rate Constant Dominance: (a) All S_{n1i} values remain positive, while S_{n2i} are negative ($i = 1, \ldots 3$), indicating opposing directional effects between parameters and state variables. (b) Synthesis rate constants (α_i) consistently exhibit stronger influence than degradation rates (β_i).

■ Time-Dependent Parameter Influence: (a) The influence of kinetic parameterson $\boldsymbol{x_1}$ **(Fig. 8)**: For $t >$ 3sec$|S_{n15}| > |S_{n13}| > |S_{n14}| \approx 0$.At transient phase ($t \leq 0.52$ sec) hierarchy shifts from $|S_{n13}| < |S_{n14}| < |S_{n15}|$(after initial equality for $t \leq 0.152$ sec).(b) The influence of kinetic parameterson $\boldsymbol{x_2}$ **(Fig. 9)**:At early phase ($t \leq 0.2$ sec)$|S_{n23}| > |S_{n24}|$ .At Mid-phase ($0.2 < t \leq 4.13$ sec) dynamic reversals occur, with $|S_{n23}|$ ultimately dominating after $t = 4.13$ sec. (c) The influence of kinetic parameterson $\boldsymbol{x_3}$ **(Fig. 10):**$|S_{n34}| > |S_{n33}|$for $t \leq 2.1$ sec, then reverse. TheS_{n33} transitions from negative to positive at $t = 0.62$ sec, whileS_{n34}remains positive.

■ Kinetic vs. Rate Parameters: Rate constants generally outweigh kinetic parameters in influence, except for S_{n34} during $t \in [0, 0.41]$ sec.

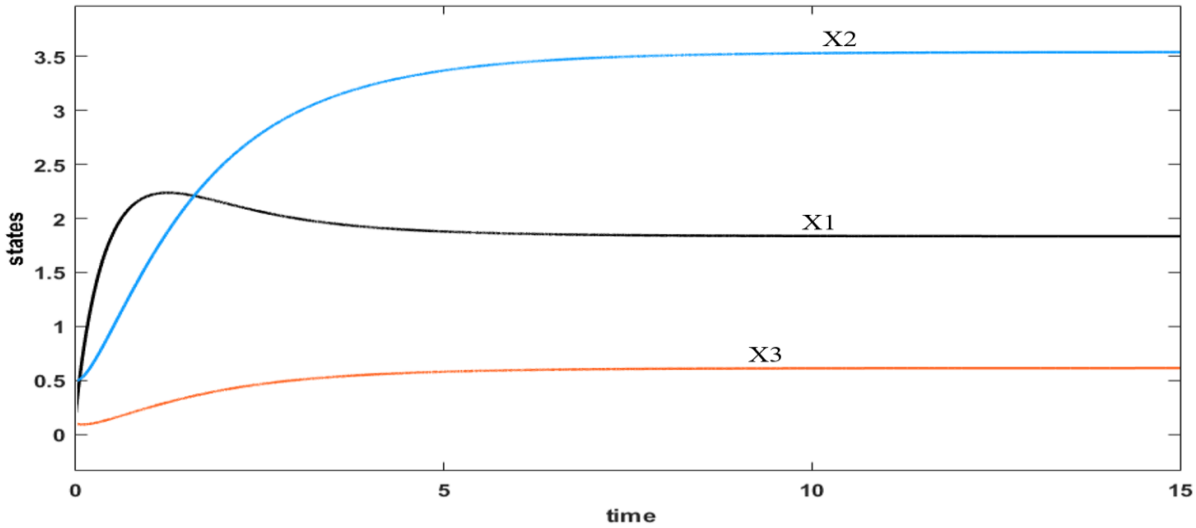

Figure 7: ($\boldsymbol{x_4}$**=0.75)**Simulation results of the system *dynamic behavior* at initial condition($\boldsymbol{x_{10}, x_{20}, x_{30}}$) = $(\boldsymbol{0.2, 0.5, 0.1})$,

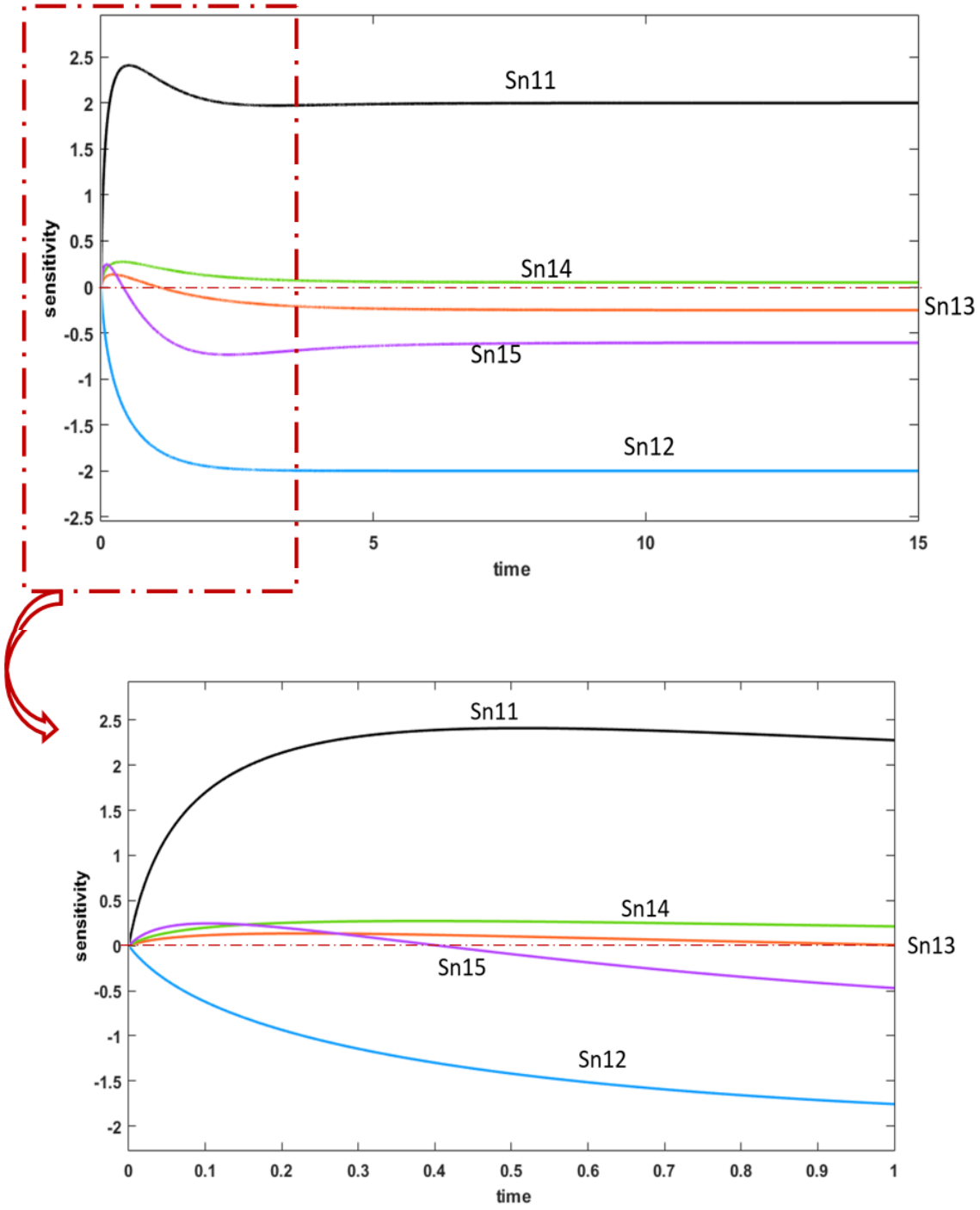

Figure 8: $((\boldsymbol{x_{10}}, \boldsymbol{x_{20}}, \boldsymbol{x_{30}}, \boldsymbol{x_4}) = (\mathbf{0.2}, \mathbf{0.5}, \mathbf{0.1}, \mathbf{0.75}))$ The dynamic sensitivity of $S_{n1i}, i = 1, \ldots 5$denote the normalized sensitivity of $x_1$to the parameters α_1 , β_1, g_{12}, g_{13}, h_{11},respectively.

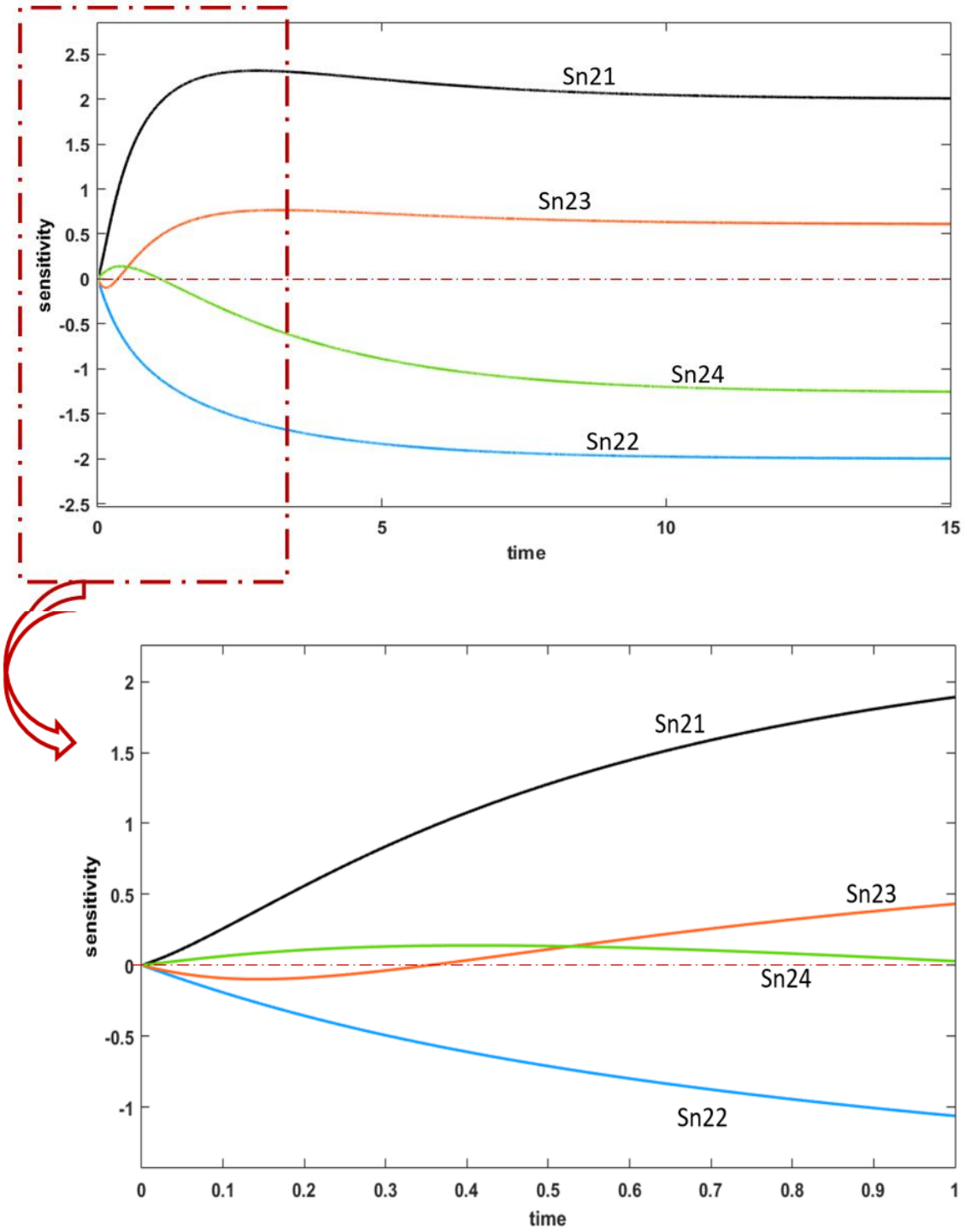

Figure 9: $((\boldsymbol{x_{10}}, \boldsymbol{x_{20}}, \boldsymbol{x_{30}}, \boldsymbol{x_4}) = (\boldsymbol{0.2}, \boldsymbol{0.5}, \boldsymbol{0.1}, \boldsymbol{0.75}))$ The dynamic sensitivity of $S_{n2i}, i = 1, \ldots 4$denote the normalized sensitivity of $x_2$to the parameters α_2 , β_2, g_{21}, h_{22},respectively.

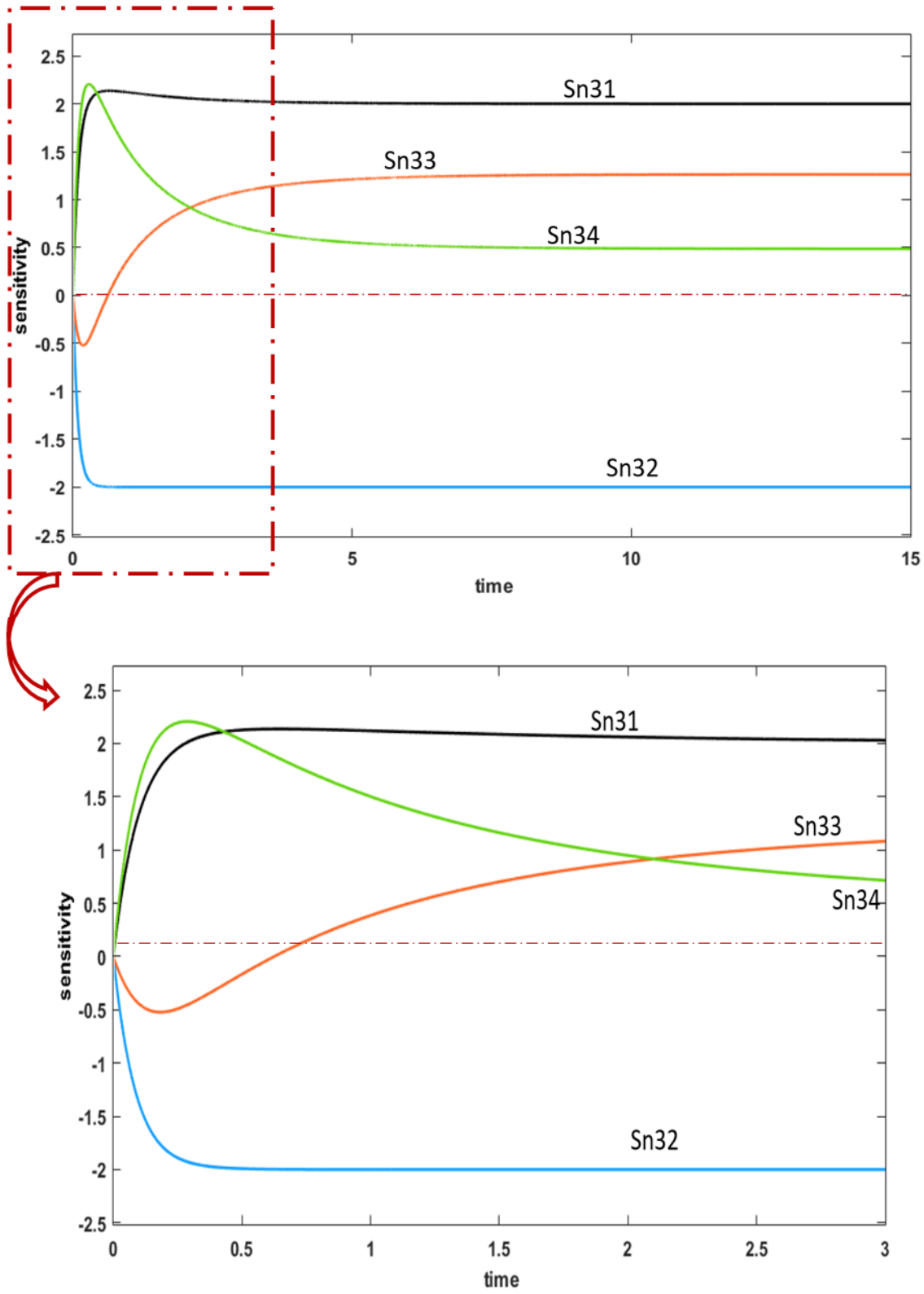

Figure 10: $((\boldsymbol{x_{10}}, \boldsymbol{x_{20}}, \boldsymbol{x_{30}}, \boldsymbol{x_4}) = (\mathbf{0.2}, \mathbf{0.5}, \mathbf{0.1}, \mathbf{0.75}))$ The dynamic sensitivity of $S_{n3i}, i = 1, \ldots 4$denote the normalized sensitivity of $x_3$to the parameters α_3 , β_3, g_{32}, h_{33},respectively.

■ **Analysis of Transient Perturbation Response Using $\mathbf{L_2}$and$\mathbf{L_1}$norm**

Our Simulink-based framework enables time-varying sensitivity analysis across all system states. To quantify the global parametric influence during transient periods ($t \in [0, t_s]$), we implement two ensemble sensitivity metrics through block-diagram operations:

L_2 Norm (Root-Mean-Square Sensitivity):

$$\|S_{nij}\| = \frac{1}{t_s}\sqrt{\int_0^{t_s}\left[S_{nij}\right]^2 dt}. \qquad (13)$$

L_1 Norm (Absolute Integrated Sensitivity):

$$IS_{nij} = \frac{1}{t_s}\int_0^{t_s}\left[S_{nij}\right] dt. \qquad (14)$$

The implementation for $S_{nij}$is visualized in Figures 12 and 13 (L_2/L_1 computation blocks) and Figures 14and 15 (detailed subsystem architectures for $\|S_n^1\|$ and IS_n^2).

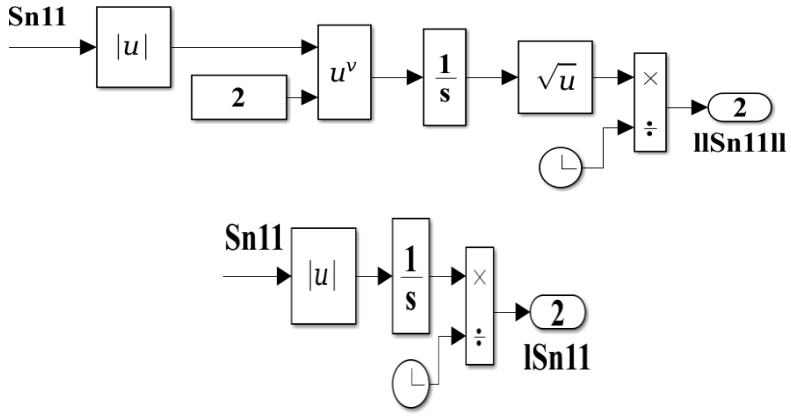

Figure 11: Visualize $||S_{n11}||$in Eq. (13) (upper figure) and IS_{n11}in Eq. (14) (down figure) in Simulink.

Under initial conditions (x_{10}, x_{20}, x_{30})= (0.2,0.5,0.1) and $x_4 = 0.75$, the system reaches steady state $(\bar{x}_1, \bar{x}_2, , \bar{x}_3)$= (1.8348, 3.5384, 0.6143) at $t_s = 10$ sec. The results of the global sensitivy are shown in bar chart (Fig. 16). For $\boldsymbol{L_2}$norm we observe that:(a) The response of $\boldsymbol{x_1}$to parameter perturbation is in the order of $\alpha_1 \approx \beta_1 \gg h_{11} > g_{12} > g_{13}$ ($||S_{n11}|| = 6.4187$, $||S_{n12}|| = 6.1047$, $||S_{n13}|| = 0.6658$, $||S_{n14}|| = 0.3431, ||S_{n15}|| = 1.9587$) . (b) The response of $\boldsymbol{x_2}$ to parameter perturbation is in the order of $\alpha_2 > \beta_2 > h_{22} > g_{21}$($||S_{n21}|| = 6.6461, ||S_{n22}|| = 5.4038, ||S_{n23}|| = 2.0858, ||S_{n14}|| = 2.6904$). (c)The response of $\boldsymbol{x_3}$to parameter perturbation is in the order of $\alpha_3 \approx \beta_3 > g_{32} > h_{33}$($||S_{n31}|| = 6.3710, ||S_{n12}|| = 6.2834, ||S_{n13}|| = 3.4729, ||S_{n14}|| = 2.75161$). For $\boldsymbol{L_1}$norm we observe that: (a) The response of $\boldsymbol{x_1}$to parameter perturbation is in the order of $\alpha_1 \approx \beta_1 \gg h_{11} > g_{12} > g_{13}$ ($IS_{n11} = 20.2431$, $IS_{n12} = 19.1395$, $IS_{n13} = 1.9869, IS_{n14} = 0.8890, IS_{n15} = 6.0289$). (b) The response of $\boldsymbol{x_2}$to parameter perturbation is in the order of $\alpha_2 > \beta_2 > h_{22} > g_{21}$($IS_{n21} = 20.6962, IS_{n22} = 16.5921, IS_{n23} = 6.3739, IS_{n24} = 7.5274$). (c) The response of $\boldsymbol{x_3}$to parameter perturbation is in the order of $\alpha_3 \approx \beta_3 > g_{32} > h_{33}$($IS_{n11} = 20.0972, IS_{n12} = 19.8271, IS_{n13} = 10.5118, IS_{n14} = 7.5805$).

Some key findings are observed. (a) *Rate constant dominates*: Forward rate constants (α_i) consistently exhibit greater influence than reverse rates (β_i) for all states (x_1, x_2, x_3). For example, For x_1, $\alpha_1 \approx \beta_1 \gg$ other parameters (L_2: 6.4187 vs 6.1047; L_1: 20.2431 vs 19.1395). (b)Kinetic parameter hierarchy:No universal dominance pattern between synthesis (g_{ij}) and degradation (h_{ij}) parameters. State-dependent variations observed that x_2 shows $h_{22} > g_{21}$ (L_2: 2.6904 > 2.0858) and x_3 exhibits $g_{32} > h_{33}$(L_2: 3.4729 > 2.7516). (c) Norm-Specific Insights:L_1 emphasizes cumulative effects (higher magnitude). L_2 better captures peak sensitivity periods.

IV. CONCLUSION

This study presents a Simulink-based framework for multiscale sensitivity analysis of S-system biological models, combining time-resolved local sensitivity (Figs. 8–10) with global ensemble metrics (L_1/L_2 norms, Figs. 16). Key advances and findings include two directions.*Unified Local-to-Global Insights*: Local dynamics reveal phase-dependent parameter dominance. Global measures integrate these effects.L_1 norms emphasize cumulative influence ($IS_{n11} = 20.24$ for α_1). L_2 norms identify peak sensitivity periods ($||S_{n21}|| = 6.65$ at $t \approx 1.2$).

Computational Contributions: Simulinkimplementation (Figs. 2-6 and Figs. 12–15) enables real-time tracking of sensitivity phase transitionsand automated computation of Jacobians (for local) and integrals (for global). The provided Simulink toolkit bridges theoretical analysis with synthetic biology design.In the future, we will use this framework to examine sloppiness and explore key design principles.

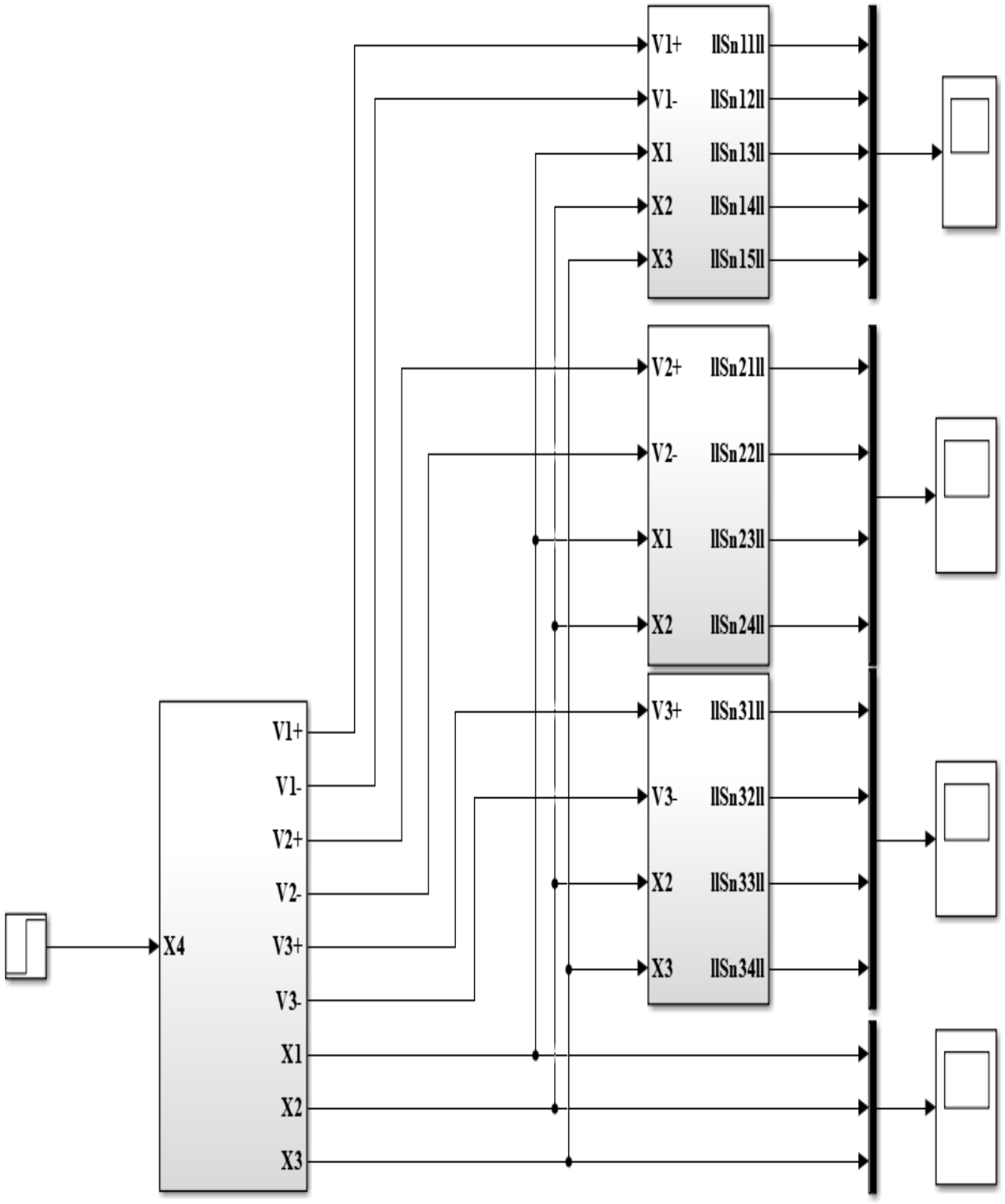

Figure 12: (***Global sensitivity***) Visualize dynamic behavior and ensemble sensitivity in$\boldsymbol{L_2}$ **norm**. The left down block runs the simulation of the reversible system ($\mathbb{S}$). The right upper block $\|S_n^1\|$,the right middle block $\|S_n^2\|$and the right down block $\|S_n^3\|$are for normalized dynamic sensitivity of x_1, $x_2$and x_3, respectively. The (Vi+, Vi-), i=1…3, denotethe forward and reverse fluxes$(v_i^+, v_i^-), i = 1 \dots 3$.

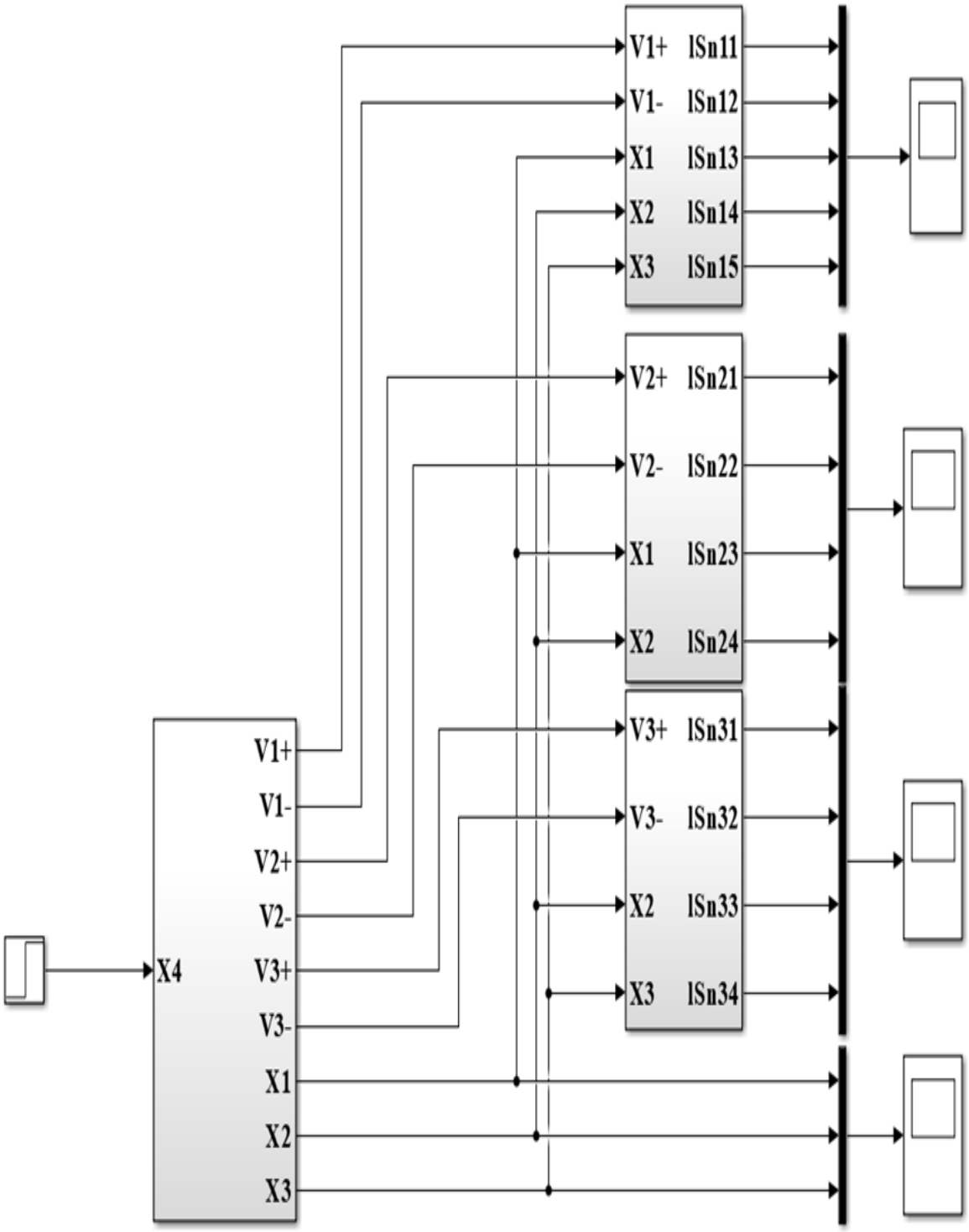

Figure 13: (***Global sensitivity***) Visualize dynamic behavior and ensemble sensitivity in$\boldsymbol{L_1}$ **norm**. The left down block runs the simulation of the reversible system (𝕊). The right upper block IS_n^1, the right middle block $IS_n^2$and the right down block $IS_n^3$are for normalized dynamic sensitivity of x_1, $x_2$and x_3, respectively. The (Vi+, Vi-), i=1…3, denotethe forward and reverse fluxes$(v_i^+,\ v_i^-), i = 1 \ldots 3$.

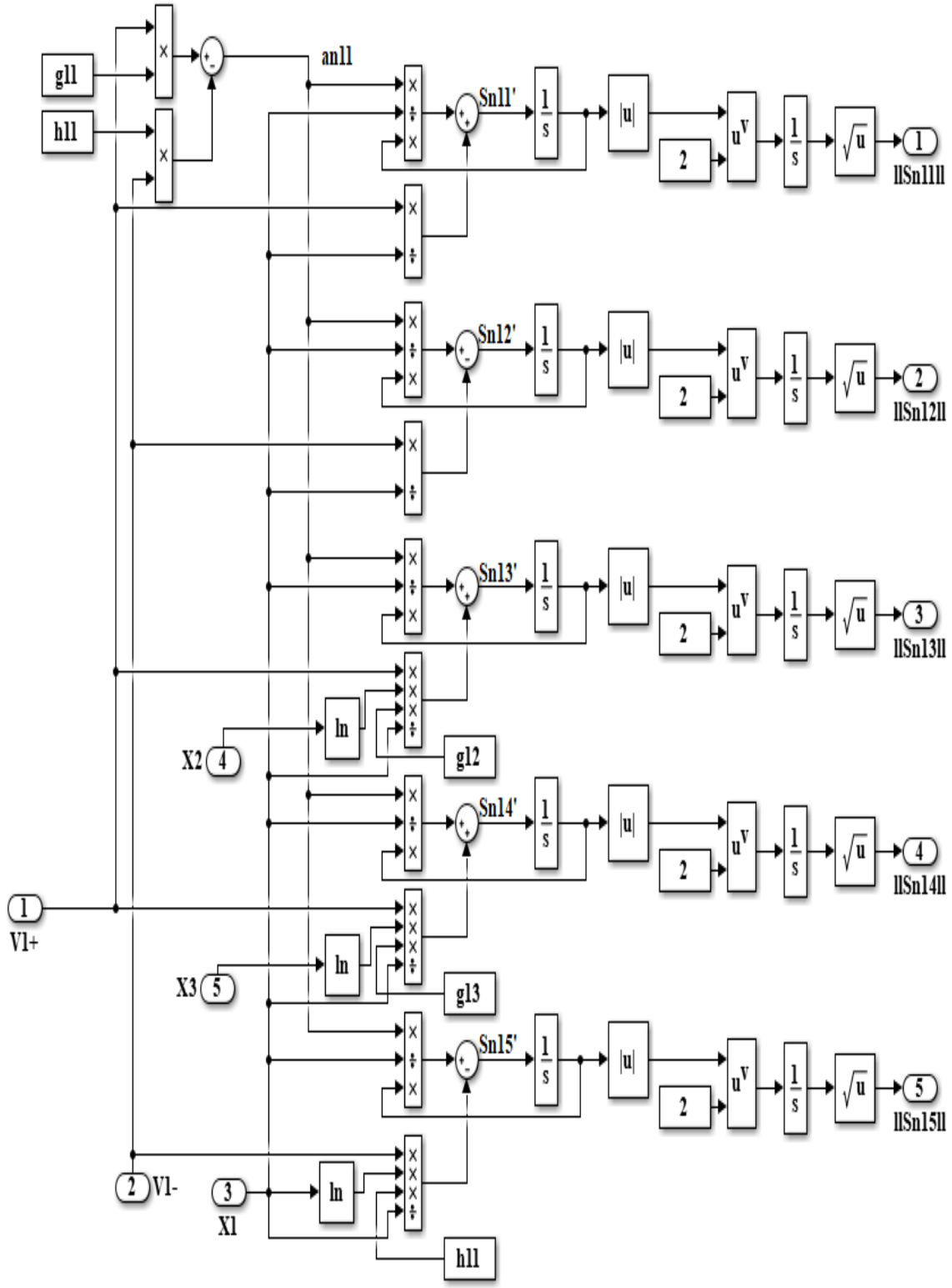

Figure 14: (***Global sensitivity***) The subsystem$\|\mathbf{S_n^1}\|$which shows in the **right upper block** of Fig. 12 for estimating theensemble sensitivity in $\boldsymbol{L_2}$ **norm**. The (Vi+, Vi-), i=1…3, denotethe forward and reverse fluxes$(v_i^+,\ v_i^-), i = 1 \ldots 3$.

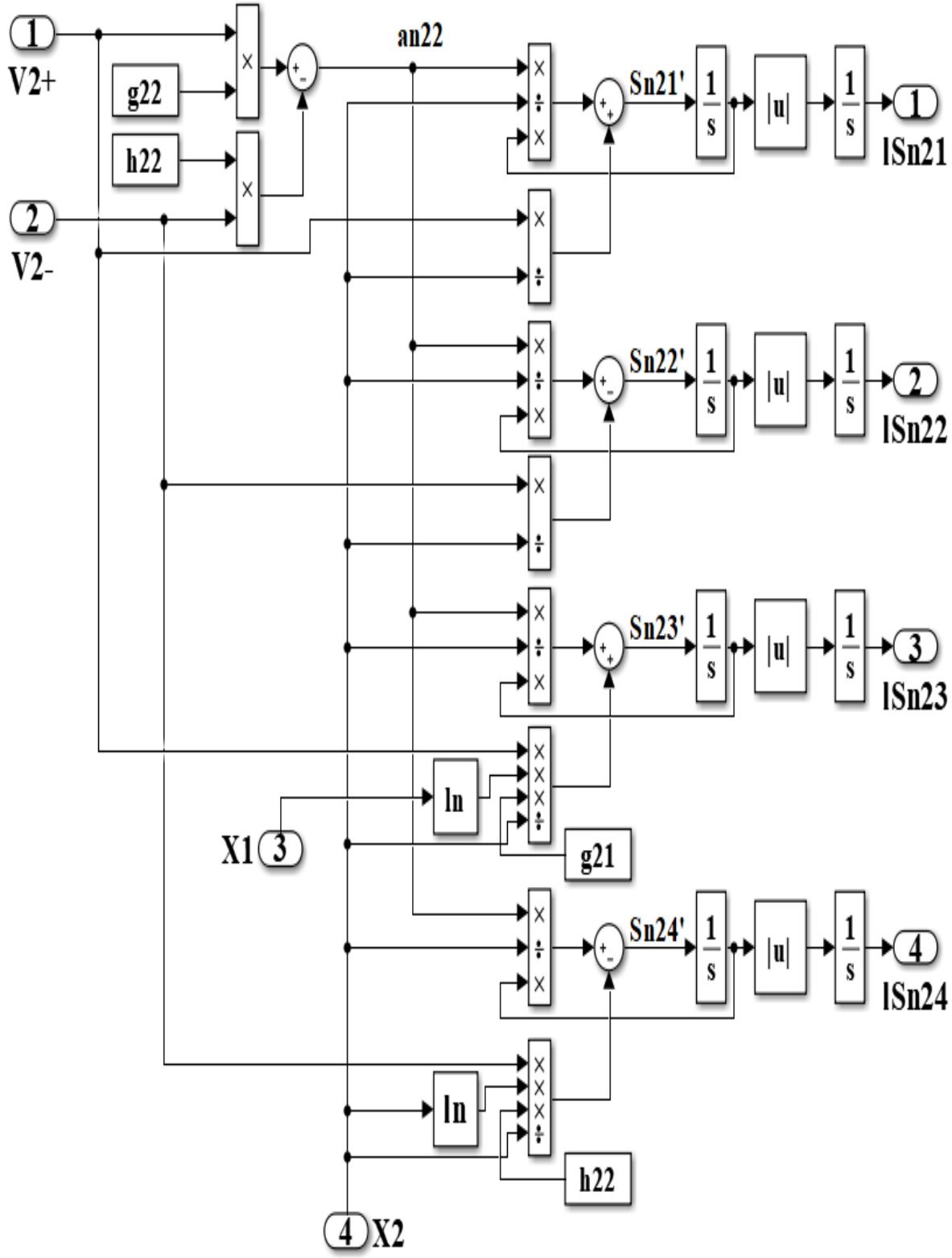

Figure 15: (***Global sensitivity***) The subsystem $\mathbf{IS_n^2}$shown in the **right middle block** of Fig. 13 for estimating theensemble sensitivity in$\boldsymbol{L_1}$ **norm**. The (Vi+, Vi-), i=1…3, denotethe forward and reverse fluxes$(v_i^+,\ v_i^-), i = 1 \ldots 3$.

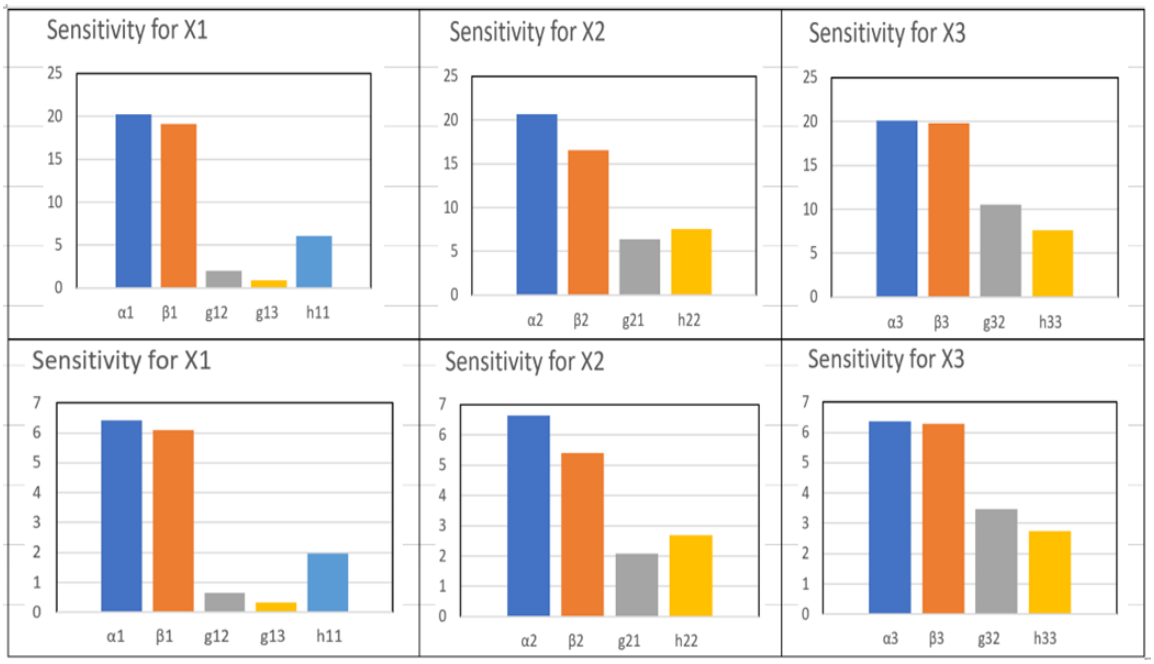

Figure 16: The global dynamic parametric sensitivity analysis. The upper three figures shows the sensitivity results in L_1 norm and the down three figures are the sensitivity in L_2norm

ACKNOWLEDGMENT

This research was supported by grant number MOST 109-2221-E-212-003from the Ministry of Science and Technology of Taiwan, R.O.C.

REFERNCES

[1]. Bartocci, E and Lió, P. (2016). Computational modeling, formal analysis, and tools for systems biology. PLoS Comput Biol 12(1): e1004591.

[2]. Sriyudthsak, K., Shiraishi, F. and Hirai, M. Y. (2016). Mathematical modeling and dynamic simulation of metabolic reaction systems using metabolome time series data. Frontiers in Molecular Biosciences, 3, 15. http://doi.org/10.3389/fmolb.2016.00015

[3]. Voit EO (**2013**) Biochemical systems theory: a review.ISRN Biomathematics.https://doi.org/ 10.1155/2013/897658

[4]. Mocek, W.T. , Rudnicki, R. and Voit, E.O. (2005) Approximation of delays in biochemical systems. Math Biosci. 198(2):190-216.

[5]. Chowdhury, A. R., Chetty, M. and Vinh, N. X. (2013) Incorporating time-delays in S-system model for reverse engineering genetic networks. BMC Bioinformatics 14:196. http://doi.org/10.1186/1471-2105-14-196

[6]. Yang, B., Bao, W., Huang, D.S. and Chen, Y. (2018) Inference of large-scale time-delayed gene regulatory network with parallel MapReduce cloud platform. Scientific Reports volume 8, Article number: 17787.

[7]. Sarode, K.D., Kumar, V.R. and Kulkarni, B.D. (2016) Inverse problem studies of biochemical systems with structure identification of S-systems by embedding training functions in a gen etic algorithm. Mathematical Biosciences 275:93–106

[8]. Wu, S. J., Wu, C. T. and Chang, J. Y. (2012) Fuzzy-based self-interactive multi-objective evolution optimization for reverse engineering of biological networks. IEEE Trans. Fuzzy Syst. 20(5): 865-882.

[9]. Wu, S.J. and Wu, C.T. (2018) Smarten up computational intelligence to decipher time series data. Applied Soft Computing 72:442-456.

[10]. Wu, S. J. and Wu, C. T. (2013) Computational optimization for S-type biological systems: Cockroach genetic algorithm. Math. Biosc. 245(2):299-313.

[11]. Wu, S. J. and Wu, C. T. (2014) Seeding-inspired chemotaxis genetic algorithm for the inference of biological systems. Computational Biology and Chemistry, 53(2): 292-307.

[12]. Wu, S. J. and Wu, C. T. (2015) A bio-inspired optimization for inferring interactive networks: cockroach swarm evolution, Expert Systems with Applications, 42(5):3253-3267.

[13]. Wu SJ. (2021) Root locus-based stability analysis for biological systems. J Bioinform Comput Biol 19(5): 2150023. https://doi.org/10.1142/S0219720021500232

[14]. Wu, C. T., Wu, S. J. and Chang, J. Y. (2013) Computational analysis of S-type biological systems. International Journal of Engineering Research and Applications, 3(1):1976-1987.
[15]. Shiraishi, F., Yoshida, E. and Voit, E. O. (2014) An efficient and very accurate method for calculating steady-state sensitivities in metabolic reaction systems. IEEE/ACM Trans. Comp. Bio. Bioinfo. 11(6):1077-1086.
[16]. Chen W, Li X, Ouyang Q, Tang C (2024). Dynamic sensitivity analysis reveals key drivers of cancer cell fate heterogeneity. Cell Systems, 15(1), 34-48.e6.
[17]. Zi Z (2021) Sensitivity analysis for dynamical systems: A biological perspective. Quantitative Biology. 9(3):257-270. (16)
[18]. Sumner T, Shephard E and Bogle IDL. (2012) A methodology for global-sensitivity analysis of time-dependent outputs in systems biology modelling. J. R. Soc. Interface 2011(4):92156–2166. http://doi.org/10.1098/rsif.2011.0891
[19]. Wang T, Wei Y and Jie. (2022) Global sensitivity analysis on debris flow energy dissipation of the artificial step-pool system, Comput Geotech 147: 104758. https://doi.org/10.1016/j.compgeo.2022.104758
[20]. Hu D, Yuan JM. (2006) Time-dependent sensitivity analysis of biological networks: coupled MAPK and PI3K signal transduction pathways. J Phys Chem A. 110(16):5361-70. doi: 10.1021/jp0561975. PMID: 16623463
[21]. Wu WH, Wang FS and Chang MS (2008) Dynamic sensitivity analysis of biological systems. BMC Bioinformatics 9:S17. https://doi.org/10.1186/1471-2105-9-S12-S17
[22]. Shiraishi F, Tomita T, Iwata M, Berrada A, Hirayama H (2009) A reliable Taylor-based computational method for the calculation of dynamic sensitivities in large-scale metabolic reaction systems: algorithm and software evaluation. Math. Biosci. 222(2):73-85. DOI: 10.1016/j.mbs.2009.09.001 PMID: 19747493
[23]. Shiraishi F, Egashira M, Iwata M (2011) Highly accurate computation of dynamic sensitivities in metabolic reaction systems by a Taylor series method. Math. Biosci. 233(1):59-67. https://doi.org/10.1016/j.mbs.2011.06.004.
[24]. Perumal TM, Gunawan R (2014) pathPSA: A dynamical pathway-based parametric densitivity snalysis. Ind. Eng. Chem. Res. 53(22):9149-9157. DOI: 10.1021/ie403277d
[25]. Sriyudthsak K, Shiraishi F (2010) Selection of best indicators for ranking and determination of bottleneck enzymes in metabolic reaction systems. Ind. Eng. Chem. Res. 49(20):9738–9742. https://doi.org/10.1021/ie100911h
[26]. Sriyudthsak K, Shiraishi F (2010) Identification of bottleneck enzymes with negative dynamic sensitivities: ethanol fermentation systems as case studies. J Biotechnol. 149(3):191-200. doi: 10.1016/j.jbiotec.2010.01.015
[27]. Sriyudthsak K, Uno H, Gunawan R, Shiraishi F (2015) Using dynamic sensitivities to characterize metabolic reaction systems. Math. Biosci. 269:153-163.
[28]. Wu SJ, Lu SY (2022) Visualize dynamic sensitivity of biological systems.Int. J. Eng. Res. Appl. 12(10):158-183.
[29]. Savageau, M. A. (1969) Biochemical systems analysis: I. Some mathematical properties of the rate law for the component enzymatic reactions. J. Theor. Biol. 25(3):365-369.
[30]. Zi, Z. (2011) Sensitivity analysis approaches applied to systems biology models. IET Syst. Biol.5(6):336-6
[31]. Thomas, P. (2022) Beyond steady-state: The Role of dynamic sensitivity in systems biology. Curr. Opin. Syst. Biol. 29:1-8. (17)
[32]. Torres NV, Voit EO (2002) Pathway analysis and optimization in metabolic engineering. Cambridge University Press.
[33]. https://www.tutorialspoint.com/matlab_simulink/matlab_simulink_tutorial.pdf
[34]. Tsai KY, Wang FS(2005) Evolutionary optimization with data collocation for reverse engineering of biological networks. Bioinformatics 21(7):1180-8.